

## Original Article

## Cardioprotective Effects of Qishen Granule (芪参颗粒) on Sarcoplasmic Reticulum Ca<sup>2+</sup> Handling in Heart Failure Rats\*

LU Ling-hui<sup>1</sup>, LI Chun<sup>2</sup>, WANG Qi-yan<sup>3</sup>, ZHANG Qian<sup>1</sup>, ZHANG Yi<sup>2,4</sup>,  
 MENG Hui<sup>2,4</sup>, WANG Yong<sup>3</sup>, and WANG Wei<sup>1</sup>

**ABSTRACT Objective:** To assess the effects of Qishen Granule (芪参颗粒, QSG) on sarcoplasmic reticulum (SR) Ca<sup>2+</sup> handling in heart failure (HF) model of rats and to explore the underlying molecular mechanisms. **Methods:** HF rat models were induced by left anterior descending coronary artery ligation surgery and high-fat diet feeding. Rats were randomly divided into sham ( $n=10$ ), model ( $n=10$ ), QSG ( $n=12$ , 2.2 g/kg daily) and metoprolol groups ( $n=12$ , 10.5 mg/kg daily). The therapeutic effects of QSG were evaluated by echocardiography and blood lipid testing. Intracellular Ca<sup>2+</sup> concentration and sarco-endoplasmic reticulum ATPase 2a (SERCA2a) activity were detected by specific assay kits. Expressions of the critical regulators in SR Ca<sup>2+</sup> handling were evaluated by Western blot and real-time quantitative polymerase chain reaction. **Results:** HF model of rats developed ventricular remodeling accompanied with calcium overload and defective Ca<sup>2+</sup> release-uptake cycling in cardiomyocytes. Treatment with QSG improved contractive function, attenuated ventricular remodeling and reduced the basal intracellular Ca<sup>2+</sup> level. QSG prevented defective Ca<sup>2+</sup> leak by attenuating hyperphosphorylation of ryanodine receptor 2, inhibiting expression of protein kinase A and up-regulating transcriptional expression of protein phosphatase 1. QSG also restored Ca<sup>2+</sup> uptake by up-regulating expression and activity of SERCA2a and promoting phosphorylation of phospholamban. **Conclusion:** QSG restored SR Ca<sup>2+</sup> cycling in HF rats and served as an ideal alternative drug for treating HF.

**KEYWORDS** Qishen Granule, Ca<sup>2+</sup> handling, heart failure, ryanodine receptor 2, sarco-endoplasmic reticulum ATPase 2a, Chinese medicine

Heart failure (HF) remains the leading cause of morbidity and mortality all over the world, despite improved prevention and treatment strategies.<sup>(1)</sup> Due to a rapidly expanding and aging population, the burden of HF is still increasing.<sup>(2)</sup> It poses investigators a challenge to uncover novel therapeutic targets for the management of HF.<sup>(3)</sup>

The defective sarcoplasmic reticulum (SR) Ca<sup>2+</sup> cycling has been shown to play crucial roles in the development of HF.<sup>(4,5)</sup> Ryanodine receptor 2 (RyR2) is the SR Ca<sup>2+</sup> release channel. Under physiological conditions, RyR2 can be phosphorylated by protein kinase A (PKA) or Ca<sup>2+</sup>/calmodulin dependent protein kinase II (CaMK II), leading to Ca<sup>2+</sup> release into cytoplasm and triggering contraction.<sup>(6-8)</sup> FKBP12.6, also known as calstabin 2, is the channel-stabilizing subunit of RyR2. In failing hearts, depleted level of FKBP12.6 and hyperphosphorylation of RyR2 destabilizes the closed state of the channel, leading to defective Ca<sup>2+</sup> leak during diastole.

Diastolic Ca<sup>2+</sup> leak reduces SR Ca<sup>2+</sup> store, impairs contractility and triggers fatal arrhythmias.<sup>(5,6)</sup> RyR2 hyperphosphorylation is associated with reduced activity of protein phosphatases (PPs), such as PP1 and PP2A, and increased activity of PKA.<sup>(5)</sup> Sarco-endoplasmic reticulum ATPase 2a (SERCA2a), also known as SR Ca<sup>2+</sup> pump, pumps Ca<sup>2+</sup> back into SR.<sup>(9,10)</sup> Phospholamban (PLB) binds to SERCA2a and inhibits its activity whereas phosphorylated

©The Chinese Journal of Integrated Traditional and Western Medicine Press and Springer-Verlag Berlin Heidelberg 2017

\*Supported by the National Natural Science Foundation of China (No. 81530100, 81470191, and 81302908)

1. School of Preclinical Medicine, Beijing University of Chinese Medicine, Beijing (100029), China; 2. Modern Research Center for Traditional Chinese Medicine, Beijing University of Chinese Medicine, Beijing (100029), China; 3. School of Life Sciences, Beijing University of Chinese Medicine, Beijing (100029), China; 4. School of Chinese Materia Medica, Beijing University of Chinese Medicine, Beijing (100102), China

Correspondence to: Prof. WANG Wei, Tel: 86-10-64286180, E-mail: [wangwei26960@126.com](mailto:wangwei26960@126.com)

DOI: 10.1007/s11655-017-2809-x

PLB (p-PLB) dissociates from the binding site of SERCA2a and relieves this inhibitory effect.<sup>(11)</sup> Reduced activity of SERCA2a may result in defects of SR Ca<sup>2+</sup> uptake in failing hearts.<sup>(5,9,11)</sup> Therefore, dysfunctions of RyR2 and SERCA2a, the two core units in cardiac excitation-contraction coupling, can lead to depletion of the Ca<sup>2+</sup> store in SR and impaired cardiac contractility.<sup>(4,5)</sup>

Chronic activation of the sympathetic nervous system is thought to be the major cause of defective SR Ca<sup>2+</sup> handling in failing hearts.<sup>(5,12)</sup>  $\beta$ -Adrenergic receptors ( $\beta$ -ARs) are activated due to elevated catecholamines, which further activate PKA pathway. The activation of PKA contributes to hyperphosphorylation of RyR2 and functional impairment of SERCA2a.<sup>(5,13)</sup> Therefore, drugs targeting neurohormonal pathways, such as  $\beta$ -blockers, might be effective in treating HF by restoring SR Ca<sup>2+</sup> handling. This hypothesis has gained accumulated evidences in a series of experimental studies.<sup>(13-15)</sup> However, the use of such drugs could be limited by their side effects and individualized therapy which requires drug titration based on blood pressure and heart rate.<sup>(16,17)</sup> Other therapies for relieving symptoms of HF, such as diuretics for pulmonary and peripheral congestion, do not halt HF progression.<sup>(18)</sup> Therefore, novel therapeutic strategies for HF remain to be investigated and Ca<sup>2+</sup> cycling proteins as well as their regulators are considered to be promising targets for the treatment of HF.

Chinese medicines (CM) have been used over centuries for treating HF in Asia and their efficacies have been proven by various studies.<sup>(19-21)</sup> Qishen Granule (芪参颗粒, QSG), an oral patent granule composed by *Radix Astragali Mongolici*, *Salvia Miltiorrhiza Bunge*, *Flos Lonicerae*, *Scrophularia*, *Radix Aconiti Lateralis Preparata*, and *Radix Glycyrrhizae*, is used routinely for treating patients with HF in China. Our previous studies have demonstrated its cardiac protective efficacies.<sup>(22-24)</sup> Network pharmacology study predicted that the potential drug targets of QSG were involved in Ca<sup>2+</sup> signaling pathway.<sup>(25)</sup> However, the mechanism of QSG in regulating SR Ca<sup>2+</sup> cycling remains poorly defined. In this study, we aimed to investigate the regulative effects of QSG on SR Ca<sup>2+</sup> leak and uptake in HF rats. This study will provide insight into developing potential therapeutic strategies in the management of HF.

## METHODS

### Drugs

Six herbs consisted in QSG were purchased from Beijing Tongrentang Pharmacy Co., Ltd. (Beijing, China) and prepared as described previously.<sup>(25)</sup> The typical chromatogram of QSG has been published in 2016.<sup>(24)</sup> Metoprolol Tartrate Tablets (batch No. 1511A08) were purchased from AstraZeneca (China) Co., Ltd.

### Animals and Modeling

Sixty male Sprague Dawley (SD) rats in specific pathogen-free grade weighing of 200 ± 20 g were purchased from Beijing Vital River Laboratory Animal Technology Co., Ltd. (license No. SCXK2012-0001). Rats were housed in temperature (20 ± 2 °C) and humidity (60% ± 5%) controlled rooms with a 12/12 h light/dark cycle. Studies were performed in accordance with the Guide for the Care and Use of Laboratory Animals published by the National Institutes of Health (NIH Publications No. 85-23, revised 1996) and with approval from the Animal Care Committee of Beijing University of Chinese Medicine.

HF models were induced by high-fat diet plus myocardial infarction (MI) surgery as described before.<sup>(26)</sup> Fifty rats were picked randomly and they were fed with high-fat diet. Seven days later, the rats underwent ligation surgery of left anterior descending (LAD) coronary artery as described before.<sup>(22)</sup> Briefly, rats were anesthetized intraperitoneally by 1% pentobarbital sodium (50 mg/kg) and ventilated via orotracheal intubation with a 16G venous indwelling cannula (TERUMO, Japan) with a tidal volume of 6.0 mL and a respiratory rate of 80 cycles/min. After exposure of heart by left thoracotomy, the LAD was ligated with a 5-0 polypropylene suture (Shuangjian, Shanghai, China) 5 mm below the left atrium. The thorax was then closed layer by layer. Twenty-four hours after ligation surgery, 34 surviving rats were divided into the following 3 groups according to complete randomized design for gavage administration: QSG group ( $n=12$ , 2.2 g/kg daily), metoprolol group ( $n=12$ , 10.5 mg/kg daily) and model group ( $n=10$ ). Three days later, electrocardiogram test showed that all surviving rats met the criteria of a successful model, marked with 6-8 deep Q-waves. The remaining 10 rats were set as sham group which received regular diet and similar procedure without actual LAD ligation. Rats

in the model group and sham group were given the same volume of distilled water. Four weeks after surgery, all rats were assessed by echocardiography and euthanized. The heart tissues and blood were harvested for further study.

### Echocardiographic Assessment

All rats underwent intraperitoneal anesthesia by 1% pentobarbital sodium (45 mg/kg) and echocardiography (Vevo 2100, Visual Sonics, Canada) was applied to assess the cardiac function and architecture. 2-D cine loops and guided M-mode frames were recorded from the parasternal short and long axis. All data were analyzed off-line with software resident on the ultrasound system. Indicators of ventricular structure, such as left ventricular internal diameter at end-diastole (LVID;d) and at end-systole (LVID;s), were measured directly. Ejection fraction (EF) and fractional shortening (FS) were calculated automatically by the software. Three cardiac cycles were picked for measurement in each rat and the mean values of the above indicators were recorded for following statistical analysis.

### Blood Lipid Measurement

Serum was extracted from fresh blood and stored at  $-20^{\circ}\text{C}$ . The levels of serum total cholesterol (TC), triglyceride (TG), high-density lipoprotein cholesterol (HDL-C) and low-density lipoprotein cholesterol (LDL-C) were detected by automatic biochemical analyzer (HITACHI 7080, Japan). The four kits were all purchased from Sekisui Medical Co., Ltd., Japan.

### Pathology Test

The new harvested hearts were crosscut 5 mm below the ligature. The upper parts of hearts were fixed in 4% paraformaldehyde for at least 48 h. After that, heart tissues were embedded in paraffin and sectioned into 5  $\mu\text{m}$  slices. Hematoxylin-eosin (HE) staining was applied to observed morphological change and sirius-red staining was applied to evaluate the degree of fibrous remodeling.

### Measurement of Intracellular $\text{Ca}^{2+}$ Concentration

The lower parts of the new harvested hearts were pruned. Tissues in the border zone of infarction area were isolated and frozen in liquid nitrogen before being transferred into  $-80^{\circ}\text{C}$  freezer for further study. Intracellular  $\text{Ca}^{2+}$  concentration of cardiac tissue was detected using calcium assay kit (C004-2, Nanjing

Jiancheng, China) according to the manufacturer's instruction. Eight samples in each group were assayed in duplicate.

### Measurement of $\text{Ca}^{2+}$ -ATPase Activity

ATPase can decompose adenosine triphosphate (ATP) to produce adenosine diphosphate (ADP) and inorganic phosphorus (Pi). ATPase level could be calculated by measuring Pi content.  $\text{Ca}^{2+}$ -ATPase activity of heart tissue was detected using ATPase assay kit (Needn't High Speed Centrifugation, A016-2, Nanjing Jiancheng, China) according to the manufacturer's instruction. Tube D in this kit is designed specifically for  $\text{Ca}^{2+}$ -ATPase. One  $\mu\text{mol}$  Pi produced by ATPase catalysis per hour per mg protein is considered as 1 ATPase activity unit [ $\mu\text{molPi}/(\text{mgprot}\cdot\text{h})$ ]. Eight samples in each group were assayed in duplicate.

### Western Blot Analysis of Protein Expressions

The frozen cardiac tissues (50 mg each) were homogenized in pre-cold lysis buffer and all samples were adjusted to the same value of protein concentration with loading buffer after being measured by a bicinchoninic acid (BCA) protein assay kit (Applygen, Beijing, China).

After being boiled for 5 min, the samples (50  $\mu\text{g}/10 \mu\text{L}$  per well) were subjected to 6% or 10% sodium dodecyl sulfate polyacrylamide gel electrophoresis (SDS-PAGE) for electrophoresis (100 V, 2 h) and then transferred to polyvinylidene fluoride membranes (Applygen, Beijing, China). The membranes were incubated with different antibodies, including SERCA2 (#9580, CST, 1:1000), PLB (#8495, CST, 1:1000), p-PLB (Ser16/Thr17, #8496, CST, 1:2000), ryanodine receptor 2 (RyR2, ab2827, Abcam, 1:1000), phosphor-RyR2 (p-RyR2, S2808, ab59225, Abcam, 1:1000), PKA (#5842, CST, 1:4000), and CaMK II (#3362, CST, 1:500) and glyceraldehyde-3-phosphate dehydrogenase (GAPDH) (ab8245, Abcam, 1:5000). After being probed with the specific horseradish peroxidase (HRP)-conjugated second antibody, the blots were treated with enhanced chemiluminescent (ECL) plus Western blotting detection reagent (GE Healthcare, UK) for 1 min at room temperature in dark room. The bands in the membrane were captured by UVP BioImaging Systems (Bio-Rad, USA) and then analyzed by Image-Lab software. The final reported data of each target protein were normalized by GAPDH.

## Real-Time Quantitative Polymerase Chain Reaction

The mRNAs of FKBP12.6, PP1 and PP2A were quantified by real-time polymerase chain reaction (RT-PCR). Specific primers were listed in Table 1. The frozen cardiac tissues were homogenized in Trizol reagent (Invitrogen, USA) and the total RNA was extracted. The RNA concentration and quality were measured using NanoDrop 2000 (Thermo Scientific, USA). And then RNAs were reverse-transcribed into cDNA using the RevertAid First Stand cDNA synthesis kit (Thermo Scientific, USA). Real-time quantitative PCR (RT-qPCR) was performed using the Applied Biosystems StepOne RT-PCR system, software v2.3, according to FastStart Universal SYBR Green Master (ROX) protocol (Roche, Germany) in 96-well microplates (Invitrogen, USA) with a total volume of 20  $\mu$ L. Fold changes were calculated by the  $2^{-\Delta\Delta CT}$  method using GAPDH as the internal control.

**Table 1. Nucleotide Sequences of Primers Used in RT-qPCR**

Primer	Accession number	Nucleotide sequences (5'-3')	Size (bp)
FKBP12.6	NM_013102.3	Forward: AACAGCACAAGCAATGGA	142
		Reverse: GCAGCACAGTAGCAGAAT	
PP1	NM_053890.1	Forward: CGTTGATTATTGAGCCAGAG	193
		Reverse: GCAGTGTGAGCATTAGTTAC	
PP2A	NM_017039.2	Forward: CGTTACCGAGAGCGTATC	159
		Reverse: CAAGGCAGTGAGAGGAAG	
GAPDH	NM_017008.4	Forward: GGATACTGAGAGCAAGAGAGA	106
		Reverse: TTATGGGGTCTGGGATGGAA	

## Statistical Analysis

All data were presented as mean  $\pm$  standard deviation ( $\bar{x} \pm s$ ) and the values were analyzed using

SPSS 17.0. Data analysis was carried out using the normal distribution test, one-way analysis of variance (ANOVA) and the Dunnett's test. Statistical significance was considered to be achieved when  $P < 0.05$ .

## RESULTS

### Effects of QSG on Echocardiography in HF Rats

Rats underwent echocardiographic evaluation 4 weeks after LAD surgery. Representative M-mode frames are shown in Figure 1A. Values of EF and FS in the model group decreased by 61.90% and 72.15% compared with those in the sham group, suggesting that HF was induced in model rats ( $P < 0.01$ ). LVID;d and LVID;s in the model group increased significantly by 51.72% and 224.19% as compared with the sham group ( $P < 0.01$ ). After treatment with QSG for 4 weeks, EF and FS values were up-regulated by 73.93% and 101.68%, and LVID;d and LVID;s were down-regulated by 14.78% and 31.26% respectively compared with those in the model group ( $P < 0.01$ ). Similarly, metoprolol treatment also improved the systolic function as well as ventricular structure (Figure 1B).

### Effects of QSG on Myocardium Structures and Fibrosis

Structures of myocardium in left ventricles were visualized by HE staining. Normal structures of myocardium were observed in the sham group, whereas myocardial cell loss, disordered arrangement of myocardium and inflammatory cell infiltration were observed in the model group. Treatment with QSG and metoprolol protected against impairment of myocardium structures caused by ischemia (Figure 2A). Sirius-red staining revealed massive collagen deposition in the model group. QSG and metoprolol treatment protected

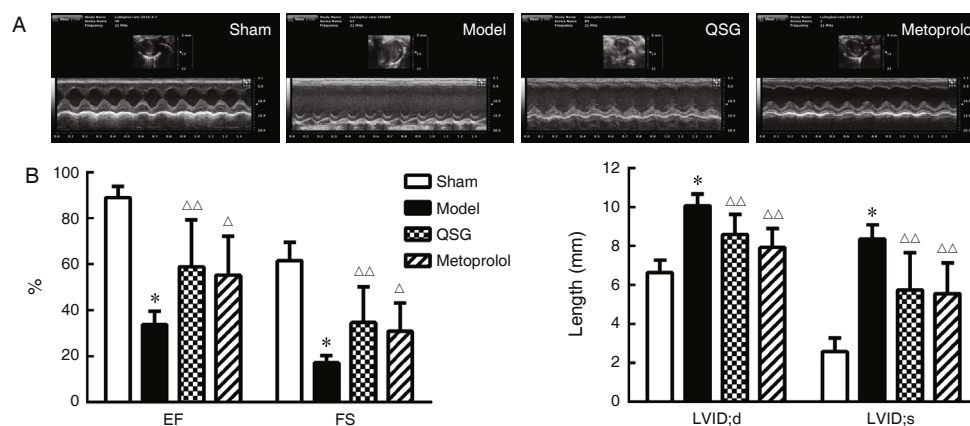


**Figure 1. Effects of QSG on Echocardiography in HF Rats**

Notes: (A) Representative images of 2D echocardiogram in four groups. (B) Echocardiographic measurements of EF, FS, LVID;d and LVID;s. \* $P < 0.01$  vs. sham group;  $\Delta P < 0.05$ ,  $\Delta\Delta P < 0.01$  vs. model group



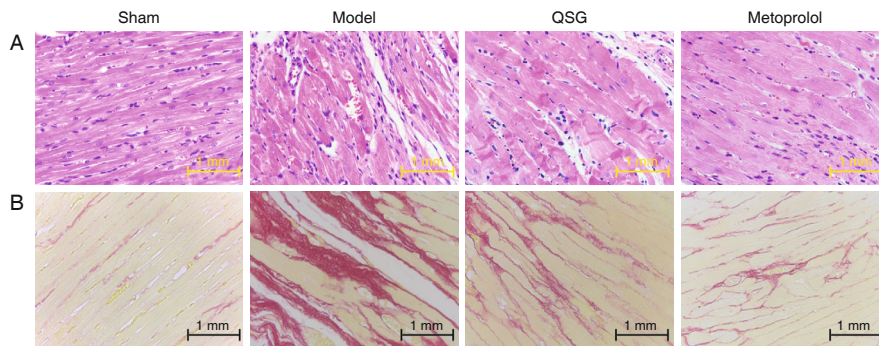


**Figure 2. Effects of QSG on Histopathological Changes in Heart Tissues of HF Rats (× 400)**

Notes: (A) HE staining; (B) sirius-red staining. Fibrous tissue was dyed red

against cardiac collagen deposition and fibrotic remodeling in heart tissues (Figure 2B).

**Effects of QSG on Blood Lipid Metabolism**

The blood levels of TC, TG and LDL-C in the model group elevated significantly by 44.92%, 223.58% and 79.88% compared with the sham group ( $P<0.01$ ). QSG treatment reduced TC level significantly by 20.08% compared with the model group ( $P<0.01$ ). Levels of TG and LDL-C were also reduced in QSG groups, though the reduction was not significant compared with the model group ( $P>0.05$ ). Metoprolol treatment showed no effect on regulating levels of TC, TG and LDL-C ( $P>0.05$ ). No significant changes were observed in levels of HDL-C in the four groups ( $P>0.05$ , Figure 3).

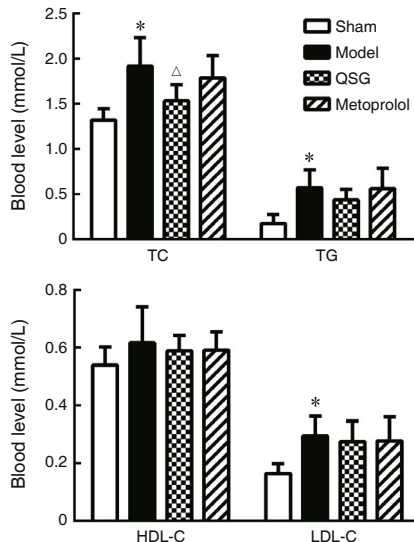


**Figure 3. Effects of QSG on Blood Lipid Metabolism of HF Rats**

Notes: \* $P<0.01$  vs. sham group;  $\Delta P<0.01$  vs. model group

**Effects of QSG on Intracellular  $Ca^{2+}$  Concentration**

The baseline level of  $Ca^{2+}$  concentration in the sham group were  $32.81 \pm 9.75 \mu\text{mol/gprot}$ , while that in the model group were elevated significantly to

$42.12 \pm 6.88 \mu\text{mol/gprot}$  ( $P<0.05$ ). Compared with model group, QSG and metoprolol treatment prevented calcium overload and maintained  $Ca^{2+}$  concentrations at levels of  $29.07 \pm 7.26$  and  $29.18 \pm 10.41 \mu\text{mol/gprot}$ , respectively ( $P<0.01$ , Figure 4 ).

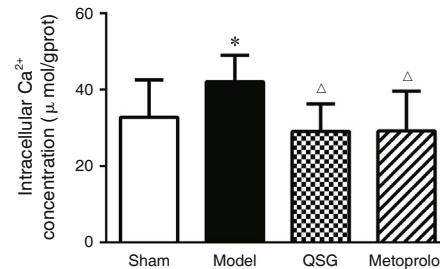


**Figure 4. Effects of QSG on Intracellular  $Ca^{2+}$  Concentration in Heart Tissues of HF Rats**

Notes: \* $P<0.05$  vs. sham group;  $\Delta P<0.01$  vs. model group

**Effects of QSG on RyR2 Leaking**

As shown in Figure 5, there were no significant differences of RyR2 protein expressions among the four groups. Expression of p-RyR2 increased by 62.47% in the model group compared with the sham group ( $P<0.01$ ). In QSG and metoprolol groups, p-RyR2 expressions were reduced by 37.01% and 46.30% respectively, compared with the model group ( $P<0.01$ ).

PKA in the model group increased by 63.00% compared with the sham group ( $P<0.01$ ). QSG treatment down-regulated expression of PKA by 11.04% compared with the model group ( $P<0.05$ ). Metoprolol had similar effect as that of QSG. There were no significant differences in protein levels of CaMK II among the four groups ( $P>0.05$ ). The transcriptional levels of PP1 and PP2A decreased by 35.38% and 40.26% in the model group compared with the sham group ( $P<0.05$ ). Compared with the model group, QSG treatment up-regulated expressions of PP1 and PP2A by 73.99% ( $P<0.01$ ) and 60.78% ( $P>0.05$ ), respectively.

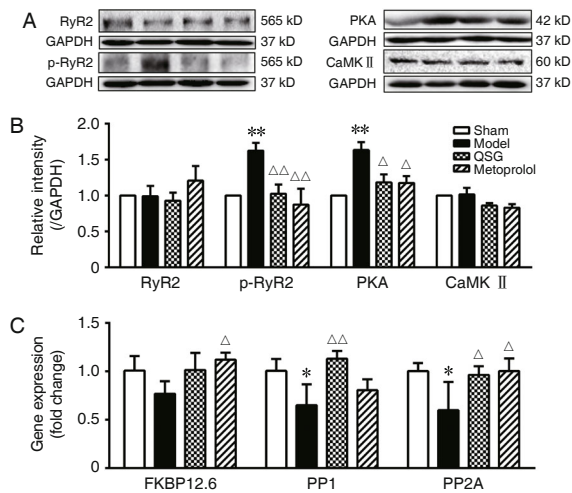


**Figure 5. Effects of QSG on RyR2 Leaking in Heart Tissue of Rats**

Notes: (A) Western blot bands of RyR2, p-RyR2, PKA and CaMK II and (B) their quantitative results in the heart tissues of rats. (C) The mRNA levels of FKBP12.6, PP1 and PP2A in hearts are quantitated and presented as the fold change. \* $P < 0.05$ , \*\* $P < 0.01$  vs. sham group;  $\Delta P < 0.05$ ,  $\Delta\Delta P < 0.01$  vs. model group

Transcription level of FKBP12.6 was suppressed in the model group and treatment with QSG elevated FKBP12.6 expression towards normal level ( $P > 0.05$ ). Metoprolol showed significant un-regulative effects on PP2A and FKBP12.6 ( $P < 0.05$ ).

### Effects of QSG on SERCA2a Uptake

Western blot results showed that the SERCA2a protein level was down-regulated by 47.08% and SERCA2a activity was reduced by 33.48% in the model group compared with the sham group ( $P < 0.05$  or  $P < 0.01$ ). QSG treatment up-regulated expressions of SERCA2a back towards normal levels and SERCA2a activity also was improved compared with model group ( $P < 0.05$  or  $P < 0.01$ , Figure 6).

There were no significant differences in protein levels of PLB among the four groups ( $P > 0.05$ ). However, protein level of p-PLB in the model group was down-regulated by 51.46%, compared with the sham group ( $P < 0.01$ ). Treatment with QSG and metoprolol up-regulated p-PLB expressions towards normal levels as compared with the model group ( $P < 0.05$ , Figure 6).

## DISCUSSION

Our previous study demonstrated that QSG treatment exerted a remarkable protective effect against cardiac dysfunction in myocardial infarction-induced HF rats.<sup>(22,23)</sup> Furthermore, drug target prediction based on network pharmacology revealed that  $Ca^{2+}$  signaling

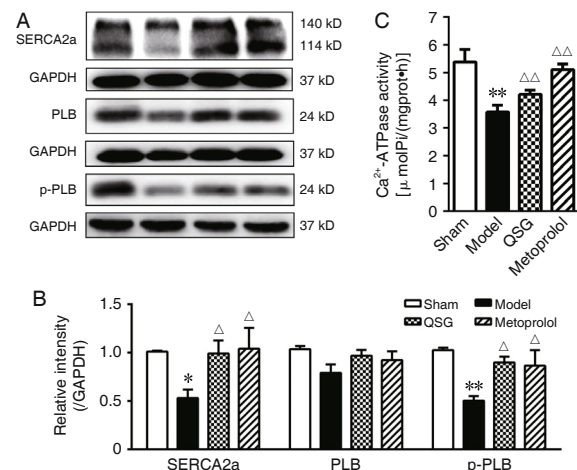


**Figure 6. Effects of QSG on SERCA2a Uptake in Heart Tissue of Rats**

Notes: (A) Western blot bands of SERCA2a, PLB and p-PLB and (B) their quantitative results. (C) SERCA2a activity was determined by measuring inorganic Pi. 1  $\mu\text{mol Pi}$  produced by ATPase per hour per mg tissue protein is considered as 1 ATPase activity unit [ $\mu\text{molPi}/(\text{mgprot}\cdot\text{h})$ ]. \* $P < 0.05$ , \*\* $P < 0.01$  vs. sham group;  $\Delta P < 0.05$ ,  $\Delta\Delta P < 0.01$  vs. model group

pathway was one of the potential targets of QSG.<sup>(25)</sup> In this study, we investigated the effects of QSG on cardiac function and structure as well as key factors involved in SR  $Ca^{2+}$  handling in HF rats. Our major findings are as follows: (1) QSG improved cardiac contractile function and reversed structural remodeling of the left ventricle in HF rats. (2) QSG attenuated calcium overload and maintained homeostasis of  $Ca^{2+}$  cycling in cardiomyocytes through regulating RyR2 channel and SERCA2a. (3) QSG down-regulated the level of p-RyR2 by inhibiting PKA and increasing PP1 expressions. (4) QSG increased expression and activity of SERCA2a and relieved the inhibitory effect of PLB on SERCA2a.

Atherosclerosis and concomitant ischemic heart disease is the most common cause of HF in developed countries.<sup>(5)</sup> Animal models induced by composite factors can simulate pathophysiological status of diseases. HF models induced by myocardial infarction superimposed on hyperlipidemia have been used widely in exploring effects and mechanisms of various drugs.<sup>(26-28)</sup> In this study, we induced a HF model of rat by LAD ligation surgery and high-fat diet feeding to investigate the effect of QSG in the treatment of HF. QSG is a CM compound consisting of 6 Chinese herbs. It has been shown that QSG possesses cardioprotective effects.<sup>(22,23,29)</sup> In this study, we confirmed that QSG improved contractive function of left ventricles in HF hearts, as evidenced by increased EF and FS. In addition, QSG treatment also protected against disruption of myocardial structure and fibrotic remodeling in HF

models. Metoprolol, one of the beta-blockers used for treating patients with HF, was applied as positive control drug in this study.<sup>(17)</sup> Metoprolol had similar cardioprotective effects as QSG. QSG administration reduced blood cholesterol level significantly, whereas metoprolol did not show lipid-lowering effect. Taken together, these results verified that QSG had cardioprotective and lipid-regulative effects in rats with HF.

Ca<sup>2+</sup> is an important messenger which mediates heartbeat through excitation-contraction coupling. In failing hearts, intracellular calcium overload due to defective SR Ca<sup>2+</sup> handling impairs mitochondrial function, leading to reduction of ATP and increased release of reactive oxygen species which in turn contributes to HF.<sup>(30)</sup> Defective Ca<sup>2+</sup> cycling in SR can be caused by excessive RyR2 leak or compromised SERCA2a uptake activity. A growing body of evidence suggests that hyperphosphorylation of RyR2 destabilizes the channel, leading to Ca<sup>2+</sup> release during diastole.<sup>(6)</sup> SERCA2a pumps cytoplasm Ca<sup>2+</sup> back to SR. Expression and activity of SERCA2a are found to be down-regulated in failing hearts and therapeutic strategies aimed at up-regulating expression of SERCA2a have been proven to be beneficial.<sup>(31,32)</sup> Restoration of SERCA2a activity is also a potential treatment strategy for HF.<sup>(9-11)</sup>

In this study, we found that intracellular Ca<sup>2+</sup> concentration of cardiac myocytes in HF model rats was much higher than that of sham controls. QSG treatment prevented calcium overload in rats that underwent ligation surgery. To explore the mechanisms by which QSG maintained Ca<sup>2+</sup> homeostasis in cardiocytes, we further investigated the related molecules involved in Ca<sup>2+</sup> release and uptake. The results demonstrated that QSG treatment stabilized Ca<sup>2+</sup> leakage by reducing phosphorylated RyR2 level. Hyperphosphorylation of RyR2 can be induced by increased activity of PKA or reduced activities of PP1 and PP2A. QSG attenuated p-RyR2 by inhibiting expression of PKA and increasing expression of PP1. Metoprolol treatment also reduced p-RyR2 level. However, expressions of FKBP12.6 and PP2A were up-regulated in the metoprolol group, suggesting that the inhibitory effect on hyperphosphorylation of RyR2 may be exerted by different mechanisms. Our data also showed that QSG treatment promoted Ca<sup>2+</sup> uptake by increasing expression and activity of SERCA2a. Expression of PLB, the endogenous inhibitor of SERCA2a, was also attenuated by QSG treatment.

In summary, our data demonstrated that ischemic injury complicated with hyperlipemia could lead to impaired SR Ca<sup>2+</sup> handling in heart. QSG treatment improved cardiac function and ameliorated ventricular remodeling in the HF model. QSG restored Ca<sup>2+</sup> homeostasis by down-regulating p-RyR2 and up-regulating activity of SERCA2a. Our findings provided insights into the cardioprotective mechanisms of QSG. Regulating key molecules in Ca<sup>2+</sup> cycling could be a potential therapeutic modality for the treatment of HF.

### Conflict of Interest

The authors declare that they have no conflicts of interest to this work.

### Author Contributions

Lu LH, Li C, Zhang Y and Zhang Q performed the experiments. Meng H performed the statistical analyses. Lu LH and Wang QY drafted the manuscript. Wang W and Wang Y designed the study, participated in its coordination and helped to draft the manuscript. Lu LH, Li C and Wang QY contribute equally to this work. All authors have read and approved the final manuscript.

### Acknowledgements

We would like to thank Prof. WU Yan and Ms. YUAN Yue-ying (Center of Scientific Experiment, Beijing University of Chinese Medicine) for the guidance on echocardiography.

## REFERENCES

1. Basra SS, Virani SS, Paniagua D, Kar B, Jneid H. Acute coronary syndrome: unstable angina and non-ST elevation myocardial infarction. *Heart Fail Clin* 2016;12:31-48.
2. Heggermont WA, Papageorgiou AP, Heymans S, van Bilsen M. Metabolic support for the heart: complementary therapy for heart failure? *Eur J Heart Fail* 2016;18:1420-1429.
3. Xanthakis V, Enserro D, Larson MG, Wollert K, Januzzi J, Quiroz R, et al. Prevalence, neurohormonal correlates and prognosis of heart failure stages in the community. *JACC Heart Fail* 2016;4:808-815.
4. Lompré AM, Hajjar RJ, Harding SE, Kranias EG, Lohse MJ, Marks AR. Ca<sup>2+</sup> cycling and new therapeutic approaches for heart failure. *Circulation* 2010;121:822-830.
5. Marks AR. Calcium cycling proteins and heart failure: mechanisms and therapeutics. *J Clin Invest* 2013;123:46-52.
6. Kushnir A, Marks AR. The ryanodine receptor in cardiac physiology and disease. *Advanc Pharmacol* 2010;59:1-30.
7. Wehrens XH, Lehnart SE, Reiken S, Vest JA, Wronska A, Marks AR. Ryanodine receptor/calcium release channel PKA phosphorylation: a critical mediator of heart failure progression. *Proceed Nat Acad Sci* 2006;103:511-518.

8. Oort RJV, Mccauley MD, Dixit SS, Pereira L, Yang Y, Respress JL, et al. Ryanodine receptor phosphorylation by calcium/calmodulin-dependent protein kinase II promotes life-threatening ventricular arrhythmias in mice with heart failure. *Circulation* 2010;122:2669-2679.
9. Park WJ, Oh JG. SERCA2a: a prime target for modulation of cardiac contractility during heart failure. *Bmb Reports* 2013;46:237-243.
10. Shareef MA, Anwer LA, Poizat C. Cardiac SERCA2A/B: therapeutic targets for heart failure. *Eur J Pharmacol* 2014;724:1-8.
11. MacLennan DH, Kranias EG. Phospholamban: a crucial regulator of cardiac contractility. *Nature Rev Molec Cell Biol* 2003;4:566-577.
12. Shan J, Betzenhauser MJ, Kushnir A, Reiken S, Meli AC, Wronska A, et al. Role of chronic ryanodine receptor phosphorylation in heart failure and  $\beta$ -adrenergic receptor blockade in mice. *J Clin Invest* 2010;120:4375-4387.
13. Reiken S, Gaburjakova M, Gaburjakova J, He KK, Prieto A, Becker E, et al. Beta-adrenergic receptor blockers restore cardiac calcium release channel (ryanodine receptor) structure and function in heart failure. *Circulation* 2001;104:2843-2848.
14. Tuncay E, Zeydanli EN, Turan B. Cardioprotective effect of propranolol on diabetes-induced altered intracellular  $Ca^{2+}$  signaling in rat. *J Bioenerget Biomembr* 2011;43:747-756.
15. Michal M, Urszula M. Effect of metoprolol and ivabradine on left ventricular remodelling and  $Ca^{2+}$  handling in the post-infarction rat heart. *Cardiovasc Res* 2008;79:42-51.
16. Dube P, Weber KT. Congestive heart failure: pathophysiologic consequences of neurohormonal activation and the potential for recovery: part II. *Am J Med Sci* 2011;342:503-506.
17. Lee HY, Baek SH. Optimal use of beta-blockers for congestive heart failure. *Circulat J* 2016;80:565-571.
18. Pellicori P, Cleland JG, Zhang J, Kallvikbacka-Bennett A, Urbinati A, Shah P, et al. Cardiac dysfunction, congestion and loop diuretics: their relationship to prognosis in heart failure. *Cardiovasc Drugs Ther* 2016;30:599-609.
19. Tang WH, Huang Y. Cardiotoxic modulation in heart failure: insights from traditional Chinese medicine. *J Am Coll Cardiol* 2013;62:1073-1074.
20. Shang H, Zhang J, Yao C, Liu B, Gao X, Ren M, et al. Qi-shen-yi-qi Dripping Pills for the secondary prevention of myocardial infarction: a randomised clinical trial. *Evid Based Complement Altern Med* 2013;2013:738391.
21. Xian S, Yang Z, Lee J, Jiang Z, Ye X, Luo L, et al. A randomized, double-blind, multicenter, placebo-controlled clinical study on the efficacy and safety of Shenmai injection in patients with chronic heart failure. *J Ethnopharmacol* 2016;186:136-142.
22. Wang Y, Li C, Ouyang Y, Yu J, Guo S, Liu Z, et al. Cardioprotective effects of Qishenyiqi mediated by angiotensin II type 1 receptor blockade and enhancing angiotensin-converting enzyme 2. *Evid Based Complement Altern Med* 2012;2012:978127.
23. Li C, Wang Y, Qiu Q, Shi T, Wu Y, Han J, et al. Qishenyiqi protects ligation-induced left ventricular remodeling by attenuating inflammation and fibrosis via STAT3 and NF- $\kappa$ B signaling pathway. *PLoS One* 2014;9:e104255.
24. Li C, Wang J, Wang Q, Zhang Y, Zhang N, Lu L, et al. Qishen granules inhibit myocardial inflammation injury through regulating arachidonic acid metabolism. *Sci Rep* 2016;6:36949.
25. Wang Y, Liu Z, Li C, Li D, Ouyang Y, Yu J, et al. Drug target prediction based on the herbs components: the study on the multitargets pharmacological mechanism of Qishenkeli acting on the coronary heart disease. *Evid Based Complement Altern Med* 2012;2012:698531.
26. Lu L, Wang J, Cao Y, Zhang Q, Li C, Wu Y, et al. Establishment and evaluation of disease and syndrome integrated animal model on coronary heart disease complicated with hyperlipemia. *China J Tradit Chin Med Pharm (Chin)* 2016;31:1816-1821.
27. Mohamed AR, El-Hadidy WF, Manna HF. Assessment of the prophylactic role of aspirin and/or clopidogrel on experimentally induced acute myocardial infarction in hypercholesterolemic rats. *Drugs R D* 2014;14:233-239.
28. Berthiaume JM, Young ME, Chen X, Mcelfresh TA, Yu X, Chandler MP. Normalizing the metabolic phenotype after myocardial infarction: impact of subchronic high fat feeding. *J Mol Cell Cardiol* 2012;53:125-133.
29. Luo L, Chen J, Guo S, Wang J, Gao K, Zhang P, et al. Chinese herbal medicine in the treatment of chronic heart failure: three-stage study protocol for a randomized controlled trial. *Evid Based Complement Altern Med* 2015;2015:927160.
30. Santulli G, Xie W, Reiken SR, Marks AR. Mitochondrial calcium overload is a key determinant in heart failure. *Proc Nat Acad Sci USA* 2015;112:11389-11394.
31. Schultz JEJ, Glascock BJ, Witt SA, Nieman ML, Nattamai KJ, Liu LH, et al. Accelerated onset of heart failure in mice during pressure overload with chronically decreased SERCA2 calcium pump activity. *Am J Physiol Heart Circulat Physiol* 2004;286:H1146-H1153.
32. Jessup M, Greenberg B, Mancini D, Cappola T, Pauly DF, Jaski B, et al. Calcium upregulation by percutaneous administration of gene therapy in cardiac disease (CUPID): a phase 2 trial of intracoronary gene therapy of sarcoplasmic reticulum  $Ca^{2+}$ -ATPase in patients with advanced heart failure. *Circulation* 2011;124:304-313.

(Received March 12, 2013; First Online May 11, 2017)

Edited by YU Ming-zhu